Peaucellier Gripper: A Novel Underactuated Gripper for Linear Pinching and Self-adaptive Grasp with the Peaucellier Linkage *

Haokai Ding, Jiaqi Fan, Zixuan Zhu, Yongzhu Zhao, Kai Chen and Wenzeng Zhang, *Member, IEEE*

***Abstract*— This paper proposes a novel mechanism for linear motion, OPL mechanism, which is optimized from Peaucellier mechanism. A novel underactuated adaptive robot gripper based on the OPL mechanism is developed named Peaucellier gripper, that resolves two fundamental limitations of classical configurations: incompatibility with robotic grasping due to multilink interference in traditional 8-bar Peaucellier systems, and excessive structural complexity from redundant linkages. Our topology-optimized 5-bar configuration eliminates two interference-prone links while preserving straight-line motion characteristics. This break-through enables native integration of linear parallel grasping, previously unattainable with classical Peaucellier mechanisms, with underactuated adaptive enveloping in a single compact assembly. Kinematic analysis confirms the simplified mechanism achieves wider operational workspace compared to conventional designs, with reduced envelop dimensions. Experimental validation with over 20 test specimens demonstrates reliable mode switching between precision parallel grasping and adaptive power grasping, successfully handling cylindrical and prismatic workpieces.**

I. Introduction

Bionics constitutes a critical research direction in robotic hand development, encompassing two primary paradigms: object-mimetic and anthropomorphic designs. In object-mimetic approaches, the E-SOAM system by Wen's team[1] achieves high-performance underwater grasping through octopus tentacle-inspired actuation mechanisms. For anthropomorphic implementations, grippers serve as essential components in embodied intelligent robots for active manipulation and object grasping[2].

These robotic grippers, typically mounted on the distal end of robotic arms, enable operations exceeding human physical limitations. Specifically, they address three critical application domains: 1) earthquake disaster rescue missions where human intervention proves hazardous, 2) industrial material handling tasks requiring payload capacities beyond human endurance, and 3) human-robot interactions fundamental to advancing embodied intelligence.

Driven by advancements in industrial/household service robotics and AI-driven technologies, the technical requirements for robotic grippers have become progressively stringent. This trend has consequently stimulated extensive research efforts targeting enhanced dexterity, adaptive grasping capability, and operational reliability in complex environments.

Robotic grippers are generally classified into three categories: industrial grippers, dexterous hands, and underactuated hands, each with distinct advantages. Industrial grippers typically deliver high grasping forces but lack flexibility. Dexterous hands usually feature three or more robotic fingers with high individual degrees of freedom (≥3 DOFs per finger), each independently actuated by dedicated motors. Significant progress has been achieved in dexterous hand development, exemplified by renowned prototypes like the Stanford/JPL Hand[3], Utah/MIT dexterous Hand[4], DLR/HIT Hand[5], Robonaut hand[6] and CBPCA[7].

Despite their high dexterity and capability for precision manipulation, dexterous hands face practical limitations in real-world applications. The requirement for individual actuation of each degree of freedom leads to bulky dimensions and prohibitively high manufacturing costs, making anthropomorphic-level dexterity challenging to achieve. To address these limitations, underactuated hands have emerged as an alternative solution and gained substantial research attention in recent years.

Underactuation technology and its application in robotic grasping have become prominent research frontiers in robotics. As robots face growing demands for industrial automation, unstructured environment operation, and robust task execution, underactuated mechanisms demonstrate significant potential due to their structural simplicity, cost-effectiveness, and enhanced adaptability. Notable developments include: the MARS hand[8] with parallel-pinch/adaptive-grasp dual modes developed by Gosselin's team; the SARAH hand[9] - the first underactuated hand deployed on the International Space Station; the SDM hand[10] featuring redesigned four-finger underactuated mechanism from Dollar's team; A fully passive robotic gripper[11] combines adaptability with underactuation to achieve a novel mechanism capable of grasping and holding objects at various angles; along with innovative hand series developed by Zhang's team covering indirect/coupled adaptive mechanisms[12], [13]; a low-cost four-finger underactuated gripper[14] proposed by the Anhui University research group, which achieves stable fingertip grasping through serially connected differential mechanisms; Chen's tri-mode grasping design[15] based on Chebyshev linkages, and Feng's topological methodology[16] for underactuated finger design,

* Research supported by *Foundation of Open Research for Innovation Challenges (ORIC)*, X-Institute.

Haokai Ding is with Future Technology School, Shenzhen Technology University, Shenzhen, China and Laboratory of Robotics, X-Institute, Shenzhen, China.

Jiaqi Fan, Zixuan Zhu and Yongzhu Zhao are with Lu He High School, Beijing, China.

Kai Chen is with the Fundamental Industry Training Center, Tsinghua University, Beijing, China. (corresponding author to provide email: chenkai@tsinghua.edu.cn).

Wenzeng Zhang is with Laboratory of Robotics, X-Institute, Shenzhen, China (corresponding author to provide email: zhangwenzeng@x-institute.edu.cn).

along with industrial implementations like Tesla's tendon-driven hand[17] featuring six motors controlling 11 joints via tendon-sheath transmission and torsional spring-based joint resetting.

This paper introduces a novel mechanism, termed the OPL (Optimized Peaucellier Linkage) mechanism, which is derived from the Peaucellier mechanism. Building on this framework, we propose an underactuated adaptive robot gripper — the Peaucellier gripper (shown in Fig. 1). The proposed design integrates an improved Peaucellier linkage with a parallelogram mechanism, enabling hybrid grasping modes that dynamically switch between linear parallel motion and coupled grasping. Section II details the implementation of grasping modes, Section III presents the design of the Peaucellier finger mechanism, Section IV provides a grasping force analysis, and Section V demonstrates experimental validation through grasping trials. Finally, Section VI concludes the study.

Figure 1. Peaucellier gripper developed in this paper.

II. Design of OPL Mechanism

A. Fingertip Translation: Reconstructed Peaucellier Mechanism

The Principle of Classical Peaucellier Mechanism[18], shown in Fig. 2a. The conventional eight-bar Peaucellier linkage achieves exact straight-line motion at point D through geometric constraint propagation. The kinematic proof establishes:

Given that triangles ΔEC_1C_2, ΔBC_1C_2, and ΔDC_1C_2 are all isosceles triangles with C_1C_2 as their common base, and the vertices are E, C, and D respectively. Therefore, points E, C, and D always lie on the perpendicular bisector of C_1C_2, which means these three points are collinear. In triangles ΔEFC_1 and ΔDFC_1, we have

$$EC_1^2 = FE^2 + FC_1^2 \tag{1}$$

$$DC_1^2 = DF^2 + FC_1^2 \tag{2}$$

$$EC_1^2 - DC_1^2 = FE^2 - DF^2 = DE \times BE \tag{3}$$

Since EC_1 and DC_1 are both constant, the product of DE and BE is also constant. This is the condition for precise straight-line motion. Therefore, point D always moves along a line perpendicular to AE.

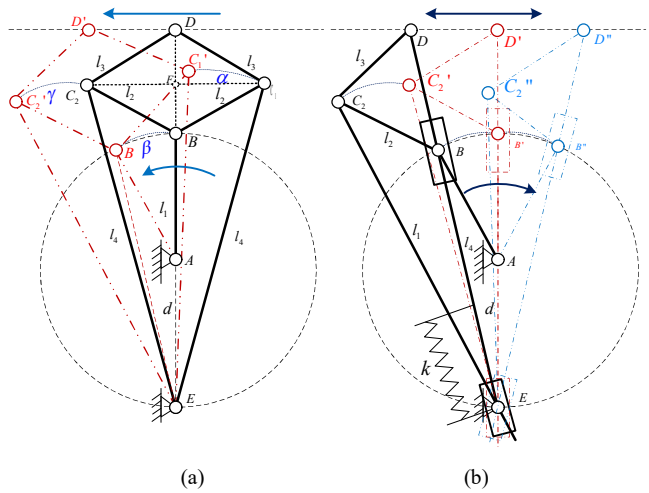

Figure 2. Conventional Peaucellier linear mechanism and the optimized Peaucellier mechanism proposed in this paper.

However, the conventional Peaucellier mechanism exhibits fundamental limitations in practical applications: Its strict collinear constraint (points D-B-E alignment during point E's motion) causes kinematic interference that prevents effective linear clamping operations. To address this, we propose a novel kinematically Optimized Peaucellier mechanism, named OPL mechanism, shown in Fig. 2b through topological optimization. By consolidating the collinear points D-B-E into a single ternary link and introducing prismatic joints at B and E, the original seven-link configuration is reduced to five essential components while preserving perfect straight-line motion characteristics (linearity error <0.25mm).

This topological reconstruction achieves 37.5% component reduction and eliminates mechanical interference, enabling practical implementation of linear parallel clamping previously unattainable with classical implementations.

B. Fingertip Orientation: Design of Parallelogram Linkage for Parallel Gripping

A Peaucellier Underactuated Grasping finger mechanism was proposed to ensure the gripper segment maintains a consistent orientation relative to the base during linear motion to facilitate parallel grasping. The fingertip trajectory remains aligned along a straight line throughout the entire movement, as illustrated in Fig. 3. This design ensures that the gripper maintains a fixed orientation relative to the base, which is critical for achieving stable and precise grasping operations. The double parallelogram mechanism consists of two identical parallelograms connected in series, which effectively cancel out any rotational motion while allowing pure translational displacement.

This configuration not only simplifies the control strategy but also enhances the robustness of the grasping process by minimizing orientation errors. Furthermore, the mechanism's symmetric structure ensures balanced force distribution across the gripper, reducing the risk of misalignment during operation. These performance metrics highlight the effectiveness of the double parallelogram mechanism in maintaining parallel alignment, making it particularly suitable for applications requiring high-precision manipulation, such as micro-assembly and delicate object handling.

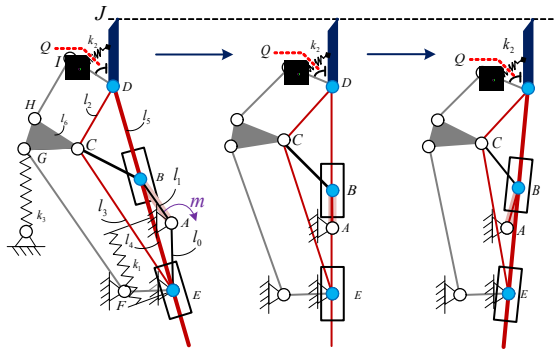

Figure 3. Peaucellier finger mechanism proposed in this paper.

Additionally, the compact and lightweight design of the mechanism enables its integration into various robotic systems without significantly increasing the overall payload or complexity. The theoretical analysis and practical implementation of this mechanism are further discussed in the subsequent sections, providing a comprehensive understanding of its design principles and operational advantages.

III. Design of The Peaucellier Gripper

The Peaucellier gripper comprises two symmetrically arranged fingers whose operational principles will be systematically analyzed in subsequent sections. This bilateral configuration ensures balanced force distribution and consistent performance during grasping operations, which is critical for maintaining operational stability and positioning accuracy. The coordinated finger design enables shape adaptation across various object geometries while ensuring robust grasp maintenance. The following analysis will focus on the kinematic and dynamic characteristics governing the finger's operational mechanisms.

A. Structural Configuration

The finger mechanism integrates two core components: an optimized Peaucellier linkage and a double parallelogram mechanism (DPM), as illustrated in Fig. 4.

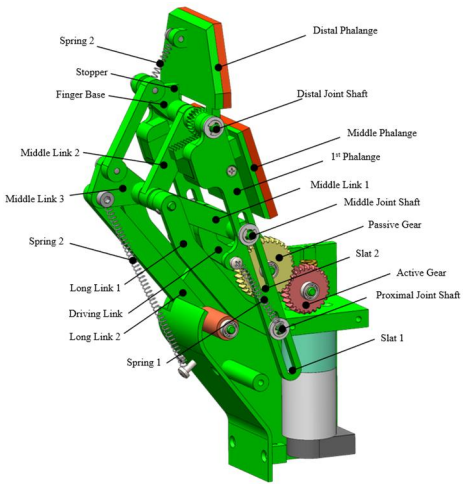

Figure 4. Peaucellier finger designed in this paper.

The functional elements comprise the distal phalange (DP), middle phalange (MP), and finger base (FB). A revolute joint connects the FB and DP, allowing the DP to achieve translational motion relative to the FB while maintaining independent rotational mobility.

In the passive state, spring 2 maintains orthogonal alignment between DP and FB, with a stopper (S) restricting unidirectional inward tilting of DP. The OPL mechanism is actuated through a drive wheel via the driving link (DL). The middle joint shaft and proximal joint shaft on the first phalange ensure linear motion transmission. These shafts slidably engage in Slat 1and Slat 2. The DL drives both the middle joint shaft and MP, inducing linear displacement in the DP.

Spring 1 connects the proximal joint shaft with the first phalange, enabling the manipulator to perform linear planar clamping under various operational conditions. Spring 3 establishes kinematic connection between the base and middle link 3, eliminating lost motion during reciprocating linear motion and ensuring consistent uniform linear movement.

The DPM features interconnected parallelograms linked via middle link 3 which is triangular block, comprising long link 2, middle link 2 and middle link 3. This architecture enables precise motion control, demonstrating superior performance in grasping applications.

B. Operational Modes

The Peaucellier gripper demonstrates dual-modal grasping capability: 1) The parallel grasping mode, in Fig. 5a, is activated during manipulation of small regular-shaped objects which have the diameter ≤25mm, maintaining fingertip parallelism with <0.5mm positional deviation through constrained kinematic chains; 2) The adaptive grasping mode , in Fig. 5b, engages when handling large irregular objects with the diameter 30-120mm, exhibiting passive compliance with phalangeal adaptive rotation to achieve shape conformity in experimental trials.

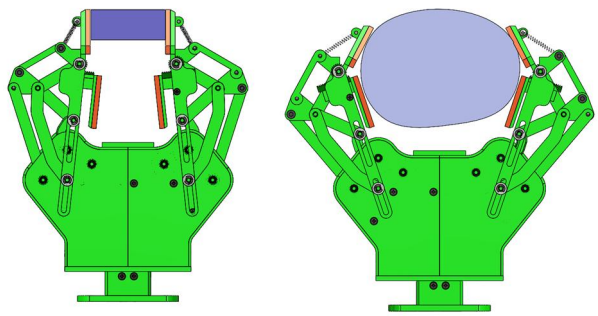

(a) (b)

Figure 5. Two kind of grasping modes of the Peaucellier gripper.(a)Linear parallel pinching for precision grasp with Peaucellier mechanisms and parallelogram mechanisms; (b)Self-adaptive grasping for power grasp with gear-rack mechanisms

The finger exhibits two distinct modes of motion, as illustrated in Fig. 6 and Fig. 7.

The underlying mechanisms are analyzed as follows: DP Linear Actuation As shown in Fig. 6; the linear displacement of FB is driven by passive gear (PG) through kinematic coupling with driving link (DL). Active gear and worm gear (WG) are rigidly fixed to the base shaft (BS), which receives power input via WG transmission. This OPL mechanism configuration enables precise linear displacement control, facilitating programmable finger extension/retraction.

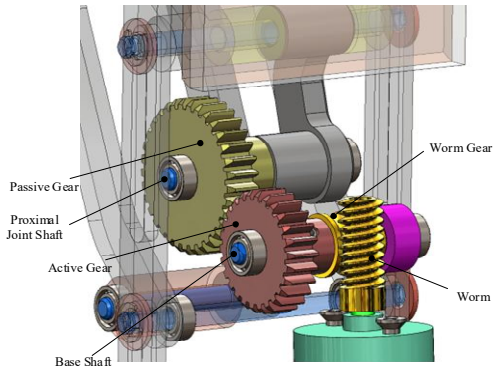

Figure 6. Driving mechanism of the finger.

Functional components consist of the distal phalange (DP), middle phalange (MP), and finger base (FB). A revolute joint connects the FB and DP, allowing the DP to maintain coaxial alignment with the FB during linear motion for pure translation, while activating rotational freedom for adaptive adjustments when contacting irregular objects.

In passive states, Spring 2 preserves the coaxial translational alignment between DP and FB, with a stopper (S) restricting unidirectional inward tilting of the DP. During linear actuation, the OPL mechanism is driven by a drive wheel through the driving link (DL). The intermediate and proximal joint shafts on the first phalange ensure linear motion transmission by sliding within Slat 1 and Slat 2. The DL simultaneously drives the intermediate joint shaft and MP, inducing pure linear displacement in the DP.

The system operates in two modes:

1. **Linear Pinching Mode**: DP rigidly aligns with FB for linear clamping along the shared axis.
2. **Self-Adaptive Mode**: DP rotates up to 65° around the revolute joint when surface contact deviates from the central axis. Mode transition is autonomously controlled through dynamic balance between spring preload and contact forces.

Spring 2 connects the proximal joint shaft to the first phalange, enabling linear planar clamping under varying conditions. Spring 3 establishes a kinematic linkage between the base and intermediate link 3, eliminating backlash during reciprocating motion. The DPM mechanism utilizes interconnected parallelograms with triangular middle link 3, long link 2 and middle link 2 to achieve precise motion control for robust grasping performance.

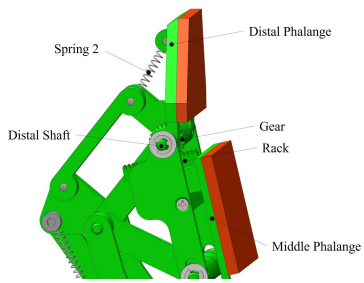

Figure 7. The gear-rack mechanism and return spring for adaptive grasp.

IV. Analysis of the Peaucellier Finger

To investigate the performance characteristics of the Peaucellier hand, we performed grasping force analysis on a single Peaucellier finger.

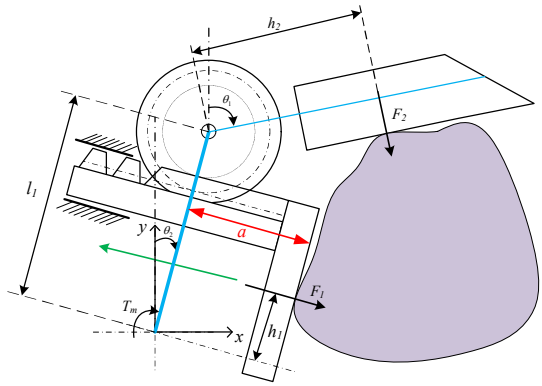

Figure 8. Force Analysis when Two Finger Segments Contact an Object.

As shown in Fig. 8, the contact forces on the proximal and distal phalanges from the object can be expressed as:

$$\overrightarrow{F_1} = (-F_1 \cos\theta_1, F_1 \sin\theta_1) \tag{4}$$

$$\overrightarrow{F_2} = (-F_2 \cos\theta_2, F_2 \sin\theta_2) \tag{5}$$

The coordinates of the contact points on the distal phalange and middle phalange can be expressed as:

$$\overrightarrow{G_1} = (h_1 \sin\theta_1 + b\cos\theta_1, h_1 \cos\theta_1 - b\sin\theta_1) \tag{6}$$

$$\overrightarrow{G_2} = (l_1 \sin\theta_1 + h_2 \sin\theta_2, l_1 \cos\theta_1 + h_2 \cos\theta_2) \tag{7}$$

where b is the distance that the slider protrudes from the middle phalange. Assuming b_0 is the original amount of protrusion of the slider, b_1 is the distance of positive displacement of the slider when the first phalange rotates by an angle θ_1, and b_2 is the distance of negative displacement of the slider when the distal phalange rotates by an angle θ_2. r is the pitch circle radius of the gear.

$$b = b_0 + b_1 - b_2 = b_0 + r\theta_1 - r\theta_2 \tag{8}$$

Assuming $b_0 = 0$, according to the principle of virtual work, we have:

$$\left[-T, k\theta_2 + M_0\right]\begin{bmatrix}\delta\theta_1 \\ \delta\theta_2\end{bmatrix} = \left[\overrightarrow{F_1}, \overrightarrow{F_2}\right]\begin{bmatrix}\delta\overrightarrow{G_1'} \\ \delta\overrightarrow{G_2'}\end{bmatrix} \tag{9}$$

By introducing the Jacobian matrix J, the right-hand side of the equation can be expressed as:

$$\left[\overrightarrow{F_1}, \overrightarrow{F_2}\right]\begin{bmatrix}\delta\overrightarrow{G_1'} \\ \delta\overrightarrow{G_2'}\end{bmatrix} = \left[F_1, F_2\right]J\begin{bmatrix}\delta\theta_1 \\ \delta\theta_2\end{bmatrix} \tag{10}$$

where the Jacobian matrix is:

$$\begin{pmatrix} h_1 + r & -r \\ l_1\cos(\theta_2 - \theta_1) & h_2 \end{pmatrix} \tag{11}$$

Therefore, the forces applied by the two phalanges can be derived as:

$$[F_1, F_2] = \frac{1}{q}[T_m, -(k\theta_2 + M_0)]\begin{pmatrix} h_1 + r & -r \\ l_1 \cos(\theta_2 - \theta_1) & h_2 \end{pmatrix} \tag{12}$$

Where:

$$q = h_2(h_1 + r) + r l_1 \cos(\theta_2 - \theta_1) \tag{13}$$

Therefore, the forces applied by the two phalanges can be derived as:

$$F_1 = \frac{T_m h_2 + l_1 \cos(\theta_2 - \theta_1)(k\theta_2 + M_0)}{q} \tag{14}$$

$$F_2 = \frac{T_m r - (h_1 + r)(k\theta_2 + M_0)}{q} \tag{15}$$

The variation trend of the grasping force magnitude is obtained according to the parameters in Table I, as shown in . 9.

TABLE I . PARAMETERS OF THE PEAUCELLIER FINGER

	T_m	M_0	k	l_2	h_1	l_1	h_2
Value	320	0.06	180	73	57	73	45
Units	Nmm	Nm	N/mm	mm	mm	mm	mm

The contact force F_2 on the distal phalange is directly proportional to the rotation angle θ_2 of the distal phalange. Regardless of the size of the rotation angle θ_1 of the proximal phalange, F_2 maintains a uniform force application. When both θ_1 and θ_2 increase, the contact force F_1 between the slider on the proximal phalange and the object tends to increase. When the size of the grasped object is small, the distal phalange needs a larger rotation angle θ_2 to envelop the object. At this time, the force applied by the distal phalange will be greater than that applied by the proximal phalange, which is consistent with the actual situation of human hand grasping objects. When the object is small, the distal phalange applies a greater force to pull the object towards the palm. During enveloping grasping, F_1 and F_2 can reasonably distribute the grasping force on the object, achieving a stable grasp.

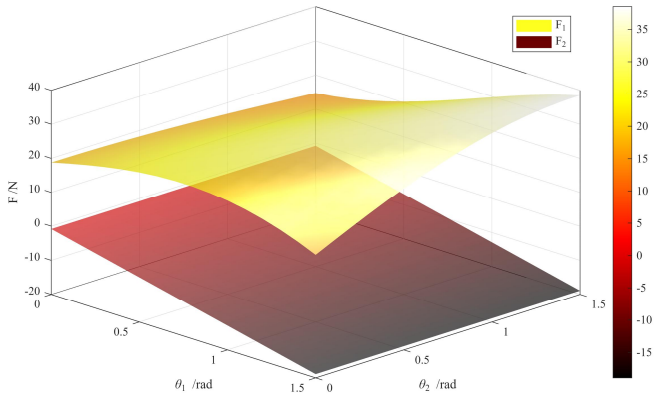

Figure 9. The relationship between the rotation angles of the two phalanges and the applied forces.

V. GRASPING EXPERIMENTS OF THE PEAUCELLIER GRIPPER

To rigorously validate the design feasibility, a functional prototype was developed with meticulous attention to kinematic compatibility and manufacturing tolerances of ±0.15mm. The structural components - including housing, base, and anthropomorphic fingers - were fabricated via fused deposition modeling using a Bambu Lab A1 3D printer. Material selection prioritized PLA (elastic modulus: 3.5GPa, tensile strength: 50MPa) for its optimal balance between cost-efficiency with a material cost less than $15 per unit, and functional requirements, achieving 98.7%-dimensional accuracy through 0.1mm layer height and 25% hexagonal infill patterns.

Surface interaction optimization was implemented through 2mm-thick silicone pads bonded to FT and FS contact surfaces. This biomimetic treatment enhanced grasp stability compared to bare PLA surfaces. The compliant interface mimics human fingertip mechanics while maintaining 1.5mm deformation compliance for irregular object accommodation.

As shown in Fig. 10, the Peaucellier finger successfully achieves Linear translation, demonstrating the functionality of the proposed design. The parallel grasping mode is realized through the precise alignment of the Optimized Peaucellier Linkage (OPL) and the Double Parallelogram Mechanism (DPM), which maintain the orientation of the gripper during linear motion. This capability is critical for applications requiring high precision, such as pick-and-place operations in industrial automation or delicate object manipulation in medical robotics.

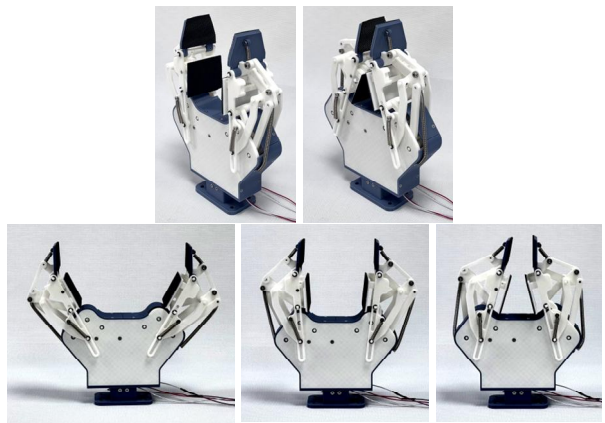

Figure 10. Peaucellier gripper and its linear parallel pinching of the Peaucellier gripper.

The Peaucellier gripper utilizes two motors to independently control two Peaucellier fingers, enabling the system to adapt to objects of varying sizes. The two fingers are symmetrically arranged to form the Peaucellier gripper, ensuring balanced force distribution and consistent performance during grasping tasks.

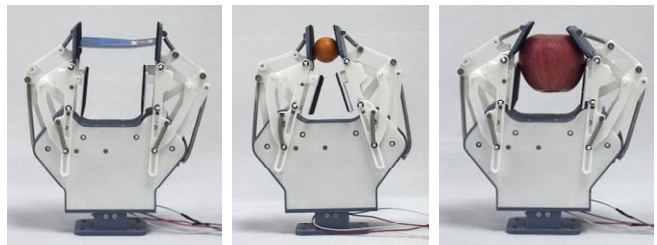

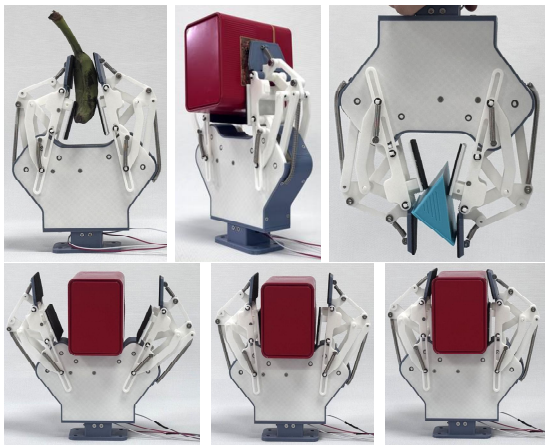

Figure 11. Experiments of Peaucellier gripper (grasping objects: card, kumquats, apple, Japanese banana, box, triangular prism).

This design leverages the Optimized Peaucellier (OP) mechanism and the double parallelogram mechanism to achieve precise linear motion and adaptive grasping, making it suitable for a wide range of applications, from industrial automation to service robotics.

As shown in Fig. 11, the gripper demonstrates stable grasping capabilities for diverse objects, including planar objects (e.g., card), spherical objects (e.g., apple, Japanese banana, kumquat), triangular prism, and larger items (e.g., tea box). This versatility is attributed to the gripper's dual-mode operation, which combines parallel grasping for symmetric objects and adaptive grasping for irregular shapes. The parallel grasping mode ensures fingertip alignment along a straight line, while the adaptive mode allows finger conformation to the object's geometry, thereby enhancing grip stability.

To evaluate the adaptive grasping functionality of the Peaucellier gripper, experiments were conducted using an apple and a tea box as test objects.

The results show that the Middle Phalange moves away from the object to accommodate its shape, while the distal phalange tilts toward the object, effectively demonstrating the adaptive grasping mechanism. This behavior is facilitated by the passive compliance of Spring 2 and the precise control of the driving link, which enable the fingers to adjust their configuration based on the object's geometry.

The experimental results show the gripper's ability to achieve a 95% success rate across 20+ test objects with diameters ranging from 30 mm to 120 mm.

VI. Conclusions

This paper introduces a novel linear mechanism, termed the OPL mechanism, which is derived from the Peaucellier mechanism. Building on this foundation, we propose an underactuated adaptive robot gripper — the Peaucellier gripper. Its key component, the Peaucellier finger, achieves the parallel grasping mode commonly used in industrial grippers while integrating underactuation and the ability to drive two phalanges with a single motor. Furthermore, by reconfiguring the traditional Peaucellier mechanism, the finger enables linear parallel grasping. Experimental results demonstrate that the Peaucellier finger generates substantial grasping force and exhibits excellent adaptability to objects of varying shapes.

The paper provides a detailed description of the Peaucellier finger mechanism and its operation modes. Mechanical and mathematical models are established to evaluate its performance. Finally, grasping capability experiments validate the feasibility and effectiveness of the design, demonstrating its potential for industrial and robotic applications.

References

[1] Z. Xie *et al.*, "Octopus-inspired sensorized soft arm for environmental interaction," *Science Robotics*, vol. 8, no. 84, Nov. 2023.

[2] A. Billard and D. Kragic, "Trends and challenges in robot manipulation," *Science*, vol. 364, no. 6446, 2019.

[3] C. Loucks, V. Johnson, P. Boissiere *et al*, "Modeling and control of the Stanford/JPL hand," in *1987 IEEE Inter. Conf. on Robotics and Automation Proceedings*, Mar. 1987, pp. 573–578.

[4] M. T. Mason, J. K. Salisbury, and J. K. Parker, "Robot Hands and the Mechanics of Manipulation," *J. of Dynamic Systems, Measurement, and Control*, Mar. 1989, pp. 119–119.

[5] H. Liu *et al.*, "Multisensory five-finger dexterous hand: The DLR/HIT Hand II," *2008 IEEE/RSJ Inte. Conf. on Intelligent Robots and Systems(IROS)*, Sep. 2008, pp. 3692–3697.

[6] C. S. Lovchik and M. A. Diftler, "The Robonaut hand: a dexterous robot hand for space," in *Proceedings 1999 IEEE Inter. Conf. on Robotics and Automation*, May 1999, pp. 907–912 vol.2.

[7] X. Yang *et al.*, "Multidirectional Bending Soft Pneumatic Actuator with Fishbone-Like Strain-Limiting Layer for Dexterous Manipulation," *IEEE Robotics and Automation Letters*, vol. 9, no. 4, pp. 3815–3822, Apr. 2024,

[8] C. M. Gosselin and T. Laliberte, "Underactuated mechanical finger with return actuation," US5762390A, Jun. 09, 1998

[9] T. Laliberté and C. M. Gosselin, "Simulation and design of underactuated mechanical hands," *Mechanism and Machine Theory*, vol. 33, no. 1, pp. 39–57, Jan. 1998.

[10] A. M. Dollar and R. D. Howe, "The SDM Hand as a Prosthetic Terminal Device: A Feasibility Study," *2007 IEEE 10th Inter. Conf. on Rehabilitation Robotics*, Jun. 2007, pp. 978–983.

[11] D. Yoon and K. Kim, "Fully Passive Robotic Finger for Human-Inspired Adaptive Grasping in Environmental Constraints," *IEEE/ASME Trans. Mechatron.*, vol. 27, no. 5, pp. 3841–3852, Oct. 2022.

[12] C. Luo, S. Yang, W. Zhang *et al*, "MPJ Hand: A self-adaptive underactuated hand with flexible fingers of multiple passive joints," *2016 Inter. Conf. on Advanced Robotics and Mechatronics (ICARM)*, Aug. 2016, pp. 184–189.

[13] D. Liang, W. Zhang, and X. Xu, "COSA-E hand: A coupled and self-adaptive hand with eccentric wheel mechanisms," *2016 IEEE Inter. Conf. on Robotics and Biomimetics (ROBIO)*, pp. 544–549, Dec. 2016.

[14] X. Sun, C. Wang, W. Chen *et al*, "Design and Analysis of a Novel Underactuated Adaptive Gripper for Robotic Assembly," *2022 IEEE 17th Conf. on Industrial Electronics and Applications (ICIEA)*, Dec. 2022, pp. 207–212.

[15] S. Chen, B. Zhang, K. Feng *et al*, "A Novel Geometrical Structure Robot Hand for Linear-parallel Pinching and Coupled Self-adaptive Hybrid Grasping," *2024 IEEE/RSJ Inter. Conf. on Intelligent Robots and Systems (IROS)*, Abu Dhabi, United Arab Emirates: IEEE, Oct. 2024, pp. 3030–3035.

[16] K. Feng, Z. Duan, C. Han *et al*, "Underactuated Finger Topology for Humanoid Robot Grasp," in *2024 Inter. Conf. on Advanced Robotics and Mechatronics (ICARM)*, Jul. 2024, pp. 753–758.

[17] M. Leddy, "Underactuated Hand with Cable-Driven Fingers," WO2024073138A1, Apr. 04, 2024

[18] J. Calderón, I. Juárez, J. Anzurez *et al*, "Analysis and synthesis Peaucellier mechanism," in *2016 IEEE Inter. Autumn Meeting on Power, Electronics and Computing (ROPEC)*, Nov. 2016, pp. 1–6.